In Vitro Assessment of the Photo(geno)toxicity Associated with Lapatinib, a Tyrosine Kinase Inhibitor

Guillermo García-Lainez,[1] Ignacio Vayá,[2,3], M. Pilar Marín,[1] Miguel A. Miranda[2,3,*] and Inmaculada Andreu[2,3,*]

[1]Instituto de Investigación Sanitaria (IIS) La Fe, Hospital Universitari i Politècnic La Fe, Avenida de Fernando Abril Martorell 106, 46026, Valencia, Spain

[2]Departamento de Química-Instituto de Tecnología Química UPV-CSIC. Universitat Politècnica de València, Camino de Vera s/n, Apdo 22012, 46071, Valencia, Spain

[3]Unidad Mixta de Investigación UPV-Instituto de Investigación Sanitaria (IIS) La Fe, Hospital Universitari i Politècnic La Fe, Avenida de Fernando Abril Martorell 106, 46026, Valencia, Spain

*Correspondence should be addressed to M. A. M. (mmiranda@qim.upv.es) or I. A. (iandreur@qim.upv.es).

ORCID M. A. Miranda: 0000-0002-7717-8750

ORCID I. Andreu: 0000-0003-3409-9443

Acknowledgements

This study was funded by the Carlos III Institute (ISCIII) of Health (Grants: PI16/01877, CPII16/00052, ARADyAL RD16/0006/0030) co-funded by European Regional Development Fund, the Spanish Government (RYC-2015-17737, CTQ2017-89416-R,) and Generalitat Valenciana Prometeo/2017/075. We would also like to thank IIS La Fe Microscopy Unit for technical assistance.

Abstract

The epidermal growth factor receptors EGFR and HER2 are the main targets for tyrosine kinase inhibitors (TKIs). The quinazoline derivative lapatinib (LAP) is used since 2007 as dual TKI in the treatment of metastatic breast cancer and currently, it is used as an oral anticancer drug for the treatment of solid tumors such as breast and lung cancer. Although hepatotoxicity is its main side effect, it makes sense to investigate the ability of LAP to induce photosensitivity reactions bearing in mind that BRAF (serine/threonine-protein kinase B-Raf) inhibitors display a considerable phototoxic potential and that afloqualone, a quinazoline marketed drug, causes photodermatosis.

Metabolic bioactivation of LAP by CYP3A4 and CYP3A5 leads to chemically reactive *N*-dealkylated (*N*-LAP) and *O*-dealkylated (*O*-LAP) derivatives. In this context, the aim of the present work is to explore whether LAP and its *N*- and *O*-dealkylated metabolites can induce photosensitivity disorders by evaluating their photo(geno)toxicity through *in vitro* studies, including cell viability as well as photosensitized protein and DNA damage. As a matter of fact, our work has demonstrated that not only LAP but also its metabolite *N*-LAP have a clear photosensitizing potential. They are both phototoxic and photogenotoxic to cells, as revealed by the 3T3 NRU assay and the comet assay, respectively. By contrast, the *O*-LAP does not display relevant photobiological properties. Remarkably, the parent drug LAP shows the highest activity in membrane phototoxicity and protein oxidation, whereas *N*-LAP is associated with the highest photogenotoxicity, through oxidation of purine bases, as revealed by detection of 8-Oxo-dG.

Keywords

Anticancer drug, Cellular Phototoxicity, DNA Damage, Metabolites, Protein photooxidation

Introduction

The epidermal growth factor receptor (EGFR) is the main target for tyrosine kinase inhibitors (TKIs). It is known that TKIs bind to tyrosine kinase ATP-binding sites and can be classified into TKIs that bind to EGFR alone or dual TKIs, which bind to both EGFR and HER2 (human epidermal growth factor receptor 2) receptors (Mendelsohn and Baselga 2000). These receptors regulate the downstream cell signaling pathways involved in cell growth, survival, and differentiation. In particular, overexpression of the HER2 is responsible for nearly 20 % of breast cancers and is associated with limited patient survival (Ding et al. 2020; Gomez et al. 2008; Spector et al. 2007).

In this context, the quinazoline derivative lapatinib (LAP) was approved by the FDA in 2007 for use as dual TKI in the treatment of metastatic breast cancer, in combination with other chemotherapeutic agents (Gavilá et al. 2020; Geyer et al. 2006; Higa and Abraham 2007; Kopper 2008; Medina and Goodin 2008). Currently, it is used as an oral anticancer drug for the treatment of solid tumors such as breast and lung cancer (Huijberts et al. 2020; Nolting et al. 2014; Schroeder et al. 2014; Wang 2014). Moreover, cytotoxic and genotoxic effects of LAP on the triplet negative breast cancer cell line MDA-MB-231 have been proven, confirming its effectiveness for the treatment of breast cancer,(Abo-Zeid et al. 2019) which is considered one of the most commonly diagnosed cancers worldwide, generally in women (Ferlay et al. 2015; Frenel et al. 2009).

Metabolic bioactivation of LAP by mainly cytochromes CYP3A4 and CYP3A5 leads to chemically reactive metabolites such as *N*-dealkylated (*N*-LAP) and *O*-dealkylated (*O*-LAP) derivatives (Towles et al. 2016).

The main side effects of LAP include hepatotoxicity, diarrhea, rash, pruritus, and nausea. In particular, LAP-induced hepatotoxicity is idiosyncratic in nature (Castellino et al. 2012; Moon et al. 2019; Rayane Mohamed 2018). It has been pointed out that the reactive metabolites may be responsible for direct or indirect toxicity to cellular proteins or DNA; however, the underlying mechanisms remain unclear (Parham et al. 2016; Spraggs et al. 2011) Moreover, it makes sense to investigate the ability of LAP to induce photosensitivity reactions bearing in mind that BRAF (serine/threonine-protein kinase B-Raf) inhibitors show a considerable phototoxic potential after exposure to UVA light (Heppt et al. 2020). Besides, it has been reported that afloqualone, a quinazoline marketed drug, causes photodermatosis as a side effect (Tokura et al. 1994).

Interestingly, we have demonstrated in previous works that drug-metabolism can result in phototoxicity enhancement (Agundez et al. 2020; Garcia-Lainez et al. 2018; Palumbo et al. 2016). In this context, Fig. 1 shows the absorption spectra of LAP, *N*-LAP, and *O*-LAP in cetyltrimethylammonium bromide (CTAB) micelles, as a model of the lipophilic environment that mimics biological membranes. As the two metabolites maintain the LAP chromophore unaltered, they also display an absorption band centered at 380 nm, which overlaps with the active fraction of sunlight able to produce photosensitivity disorders.

With this background, the goal of the present work is to explore whether LAP and its *N*- and *O*-dealkylated metabolites have the capability to induce photosensitivity disorders. This has been achieved through evaluation of their photo(geno)toxicity by means of *in vitro* studies, including cell viability as well as photosensitized protein and DNA damage.

Materials and methods

General Reagents

All solvents were of the highest grade commercially available. Chlorpromazine hydrochloride (CPZ; CAS 69-09-0), sodium dodecyl sulphate (SDS; CAS 151-21-3) and Lapatinib (LAP; CAS 231277-92-2) were purchased from Sigma-Aldrich (Madrid, Spain). N-De [N-De [2-(methylsulfonyl) ethyl] lapatinib (*N*-LAP, CAS 697299-82-4) and O-De (3-fluorobenzyl) lapatinib ditosylate salt (*O*-LAP; CAS 1268997-70-1) were provided by Santa Cruz Biotechnology (Dallas, USA) and Toronto Research Chemicals (North York, Canada), respectively. LAP, *N*-LAP and *O*-LAP stock solutions were prepared in DMSO as vehicle, whereas CPZ and SDS were dissolved in ultrapure water (Milli-Q®). Plasmid pBR322 was purchased from Roche Diagnostics (Barcelona, Spain) and low melting point agarose was provided by Pronadisa (Madrid, Spain). SYBR™ Safe and SYBR™ Gold DNA stains were supplied by Invitrogen (Madrid, Spain). DNA repair enzyme T4 endonuclease V (Endo V) was provided by Werfen (Barcelona, Spain) and DNA repair enzymes endonuclease III (Endo III) and *E coli* formamidopyrimidine DNA glycosylase (FPG) were from Sigma-Aldrich. Culture cells genomic DNA extraction kit was purchased from Neo-Biotech (Nanterre, France). For cell culture experiments, Dulbecco's Modified Eagle Medium (DMEM), fetal bovine serum (FBS), and penicillin-streptomycin (1.0×10^5 U/mL, 1.0×10^5 µg/mL) were supplied by Invitrogen. Trypsin-EDTA (0.25%–0.02%) and glutamine (100 mM) solutions were provided by Cultek

(Madrid, Spain). Phosphate buffered saline buffer (PBS; 0.01 M, pH 7.5), neutral red dye, Human Serum Albumin (HSA) and protein carbonyl content assay kit was obtained from Sigma-Aldrich. Reagent kits for single cell electrophoresis assay and 8-Oxo-dG Elisa were provided by Trevigen (Barcelona, Spain). CellMask™ Orange Plasma membrane stain was supplied by Invitrogen and mowiol by Calbiochem.

Cell culture conditions

BALB/c 3T3 mouse fibroblast cell line and human skin fibroblasts (FSK) were cultured in 75 cm^2 plastic flasks in DMEM supplemented with 10% FBS, 4mM L-Glutamine and penicillin/streptomycin (100 U/mL, and 100 µg/mL) in a humidified incubator (100% relative humidity) at 37ºC under 5% CO_2 atmosphere. Cells were routinely passed twice a week (1:4 and 1:10 splitting ratios for FSK and 3T3 cells, respectively) and viability of the cultures was checked by trypan blue exclusion assay before each experiment.

Absorption and emission spectra measurements

Absorption spectra were recorded in a JASCO V-760 spectrophotometer. For fluorescence experiments, 5 µM of LAP, *O*-LAP and *N*-LAP in DMEM were incubated for 1 h in black 96-well plates in the presence of FSK cells (8.000 cells/well). Fluorescence spectra (λ_{exc} = 320 nm) were recorded using a Synergy H1 multi-mode microplate reader.

Cellular localization by confocal microscopy

Fibroblast cells were seeded on glass coverslips in 24 well-plates (5.0×10^4 cells/well). Next day, DMEM medium was replaced by 500 µL of drug solutions (LAP, *N*-LAP or *O*-LAP) at 5 µM containing CellMask™ Orange Plasma membrane stain (dilution 1:20000) and incubated for 30 min at 37ºC. Then, coverslips were washed twice for 5 min with PBS and finally mounted with mowiol. Microcopy and imaging were performed with a Leica SP5 confocal microscope using sequential mode. The excitation wavelengths were 405 nm for LAP, *N*-LAP and *O*-LAP and 543 nm for CellMask™ Orange Plasma membrane and maxima emission wavelengths were 450 and 567 nm, respectively. Representative images were selected from at least three different regions on the slide.

Irradiation equipment

All UVA irradiations were carried out with an LCZ-4 photoreactor fitted with six top and eight sides Hitachi lamps (λ_{max} = 350 nm, Gaussian distribution; Luzchem, Canada), which emit 94% UVA radiation and 2% UVB radiation. Samples were irradiated using 96-well transparent plates for the *in vitro* 3T3 NRU phototoxicity assay and photosensitized damage to plasmid DNA assay and 24-well transparent plates for the

protein photooxidation assay, comet assay and 8-Oxo-dG determination assay. The irradiations were performed through the lid of the plates which does not absorb beyond 310 nm. This mitigates the direct effect of UVB radiation over the cell cultures. In photogenotoxicity experiments, the cell viability of cultures after irradiation was higher than 85%, indicating the suitability of the UV dose to avoid false-positive results triggered by DNA fragmentation due to cell death. In all experiments, in order to avoid overheating plates were kept on ice inside the photoreactor during the irradiation step and the temperature remained under control by ventilation.

In vitro 3T3 neutral red uptake (NRU) phototoxicity assay

The *in vitro* 3T3 NRU phototoxicity test was carried out following the OECD Guideline 432 (OECD 2004). with minor modifications described in Garcia-Lainez *et al*.(Garcia-Lainez et al. 2018) CPZ and SDS were used as the positive phototoxic and negative non-phototoxic control, respectively. In brief, for each compound two 96-well plates seeded at a density of 2.5×10^4 cells/well. Next day, 3T3 cells were incubated with test compounds (LAP, *N*-LAP and *O*-LAP) at 8 concentrations ranging from 0.1 µM to 100 µM for an hour in dark conditions. Afterwards, one plate was irradiated on ice for 12 minutes with a non-cytotoxic dose of UVA equivalent to 5 J/cm^2 whereas the other was kept in a dark box. Later, compound solutions were replaced with freshly DMEM medium and plates were further incubated overnight. After that time, neutral red solution (50µg/mL) was added into the wells and incubated for 2h at 37ºC. Cells were then washed once with PBS and neutral red was extracted from lysosomes in 100 µL of the extraction buffer (distilled water 50% (v/v), ethanol 49.5% (v/v) and acetic acid 0.5% (v/v). Finally, absorbance was read at 540 nm on a Synergy H1 microplate reader. For each compound dose-response curves were established to determine the concentration reducing a 50% the neutral red uptake (IC50) in dark and UVA Light conditions. Afterwards, photoirritation factor (PIF) values were calculated using the subsequent equation: $PIF = \frac{\text{IC50 DARK}}{\text{IC50 UVA LIGHT}}$. According to OECD Guideline 432, a compound is labelled as "non-phototoxic" when PIF is < 2, "probably phototoxic" if PIF is between 2 and 5 and "phototoxic" if PIF is > 5.

Protein photooxidation assay

Solutions of HSA (5 mg/ml, 1 mg protein/sample) in PBS were prepared and irradiated alone or in the presence of 30 µM of LAP, *O*-LAP or *N*-LAP with an UVA dose of 15 J/cm^2 as described above. Immediately after irradiation, the extent of HSA oxidation in

all samples was measured spectrophotometrically by incubation during 10 min with 100 µL of 2,4-dinitrophenylhydrazine (DNPH) at room temperature in order to form stable dinitrophenyl hydrazone adducts. After incubation, proteins were precipitated by the methanol/chloroform method followed by its re-solubilization in guanidine buffer (6 M). Finally, absorbance at 375 nm was recorded using the Synergy H1 microplate reader and the HSA oxidation degree was expressed as nmol of carbonyl per mg protein.

Photosensitized damage to plasmid DNA

Samples containing the drug (LAP) or its metabolites (30µM) in PBS with 1 mg/mL HSA and 250 ng of supercoiled pBR322 were prepared. Then, mixtures were either kept in dark conditions or irradiated during 30 minutes (15 J/cm^2). Immediately after irradiation, loading buffer (0.25% bromophenol blue, 30% glycerol, in water) was added to each sample. In order to reveal the nature of the DNA damage, DNA-repair enzymes experiments were also performed. To this purpose, after the irradiation step samples were digested with an excess of Endo V, Endo III or FPG (0.5 U) at 37ºC for 1h and then, loading buffer added as detailed above. Next, all samples were loaded on a 1% agarose gel containing SYBR® Safe as nucleic acid stain. The electrophoresis was run in TAE Buffer (0.04 M Tris-acetate, 1 mM EDTA) at 100 V for 1h. Finally, the agarose gels were visualized with the Gel Logic 200 Imaging System (Kodak) and the intensity of Form I (supercoiled) and Form II (nicked relaxed) bands was quantified using the Image-J software. Finally, the relative amount of the Form II of the plasmid was calculated.

Nuclear DNA damage by Single Cell Gel Electrophoresis (comet) assay

Single cell gel electrophoresis assay (comet assay) was performed as previously described by Garcia-Lainez *et al.*(Garcia-Lainez et al. 2018) to allow the detection of both single and double strand breaks and alkaline labile sites on nuclear DNA. Thus, FSK cell cultures in exponential growth were trypsinized, resuspended in cold PBS and placed on the ice during 2 h as trypsin detachment induces mild DNA damage in FSK cell line. Then, two 24-wells plates (1.0×10^5cells/well) were seeded and treated with 30 µM of LAP or its metabolites (*N*-LAP or *O*-LAP) for 1h at 37ºC in darkness. CPZ (10µM) was used as the reference photogenotoxic control of this assay. After incubation, one plate was placed in the photoreactor to irradiate the cells (2.5 J/cm^2) and the other one was kept in darkness as negative control. Later, irradiated and non-irradiated cells were harvested from plates and mixtures of 100 µL of cell suspension (2.0×10^4 cells) and 100 µL of 1% low melting point agarose solution were prepared and loaded onto Trevigen ® treated slides. Slides were placed on ice-cold tray to allow drop jellification. Afterwards, slides

were immersed in coupling jars with lysis buffer (2.5 M NaCl, 0.1 M Na_2EDTA, and 0.01 M Tris, 1% TritonX-100, pH 10) to promote cell lysis and incubated overnight at 4ºC. Next day the Trevigen ® comet assay electrophoresis tank was loaded with slides, filled with 850 mL cold alkaline electrophoresis buffer (0.2 M NaOH, 1 mM EDTA in distilled water and pH ≥13) and let during 40 min for DNA unwinding at 4ºC. The electrophoresis was run at 21 V (1 V/cm) for 30 min at 4ºC and then the slides were washed twice in PBS for 5 min. DNA fixation was achieved by two subsequent incubations in 70% ethanol and 100% ethanol solutions during 5 min and air-dried. Nuclear DNA was stained with a SYBR Gold® (1:10.000 TE buffer) bath for 30 min, air-dried and kept in darkness until its visualization. Visualization of nucleoids and tails of the samples was carried out with a Leica DMI 4000B fluorescence microscope. For each sample at least 5 pictures were taken. Finally, DNA damage of each sample was calculated for each condition analyzing at least 100 DNA comets by visual scoring. Total comet score (TCS) was determined with the classification of 6 DNA damage categories (Møller, 2006) with the following formula: [(Nclass 0 comets × 0) + (Nclass 1 comets × 1) + (Nclass 2 comets × 2) + (Nclass 3 comets × 3) + [(Nclass 4 comets × 4) + (Nclass 5 comets × 5) + (Nclass 6 comets × 6)]/6 and expressing results in 1–100 arbitrary units, where class 0 comets are comets with no DNA damage and class 6 comets indicate comets with maximum DNA damage.

Assessment of 8-Oxo-dG as a biomarker of oxidative DNA damage

In this experiment, FSK cells were seeded in two 24-well plates at a density of 7.5×10^5 cells/well and treated with 30 µM of LAP, *N*-LAP or *O*-LAP for 30 min at 4ºC in dark conditions. Then, one plate was irradiated with an UVA dose equivalent to 2.5 J/cm^2 and the other one was kept in dark conditions as negative control. Immediately, cells were harvested and genomic DNA extraction was performed in all samples according to the manufacturer's protocol. Purified DNA was quantified with a Nanodrop 2000c (Thermo Scientific) and the ratio A260/A280 was between 1.8 and 2.0. Next, 2 µg DNA (100 ng/mL) was digested with DNase I (1 U) at 37ºC for 1h, followed by alkaline phosphatase incubation (1 U) at 37ºC for 1h. Finally, 8-Oxo-dG concentration was determined in all samples by a competitive ELISA assay following the manufacturer's instructions interpolating from the standard curve the sample concentration. Data were expressed in nanomoles of 8-Oxo-dG formed.

Data analysis and statistics

Results are presented as mean ± standard deviation obtained from the results of at least three independent experiments unless indicated otherwise. Data were analyzed and

regression methods developed using the GraphPad software. Statistical significance was assessed by the t-Student test and p values lower than 0.05 were considered significant (*p<0.05; **p<0.01; ***p<0.001).

Results and Discussion

In vitro cellular uptake of LAP and its metabolites

Intracellular localization of LAP and its *N*- and *O*-dealkylated metabolites was analyzed by confocal microscopy using their intrinsic fluorescence properties. Following 30 min of incubation, the efficient uptake of all compounds by the cells was observed. Despite differences in their fluorescence intensity, it was not observed a predominant particular distribution in any organelle (Fig. 2a). Fluorescence emission spectra (λ_{exc}= 320 nm) of LAP, *N*-LAP and *O*-LAP were recorded after internalization on FSK cells (Fig. 2b). Thus, LAP showed a maximum emission around 450 nm, for *N*-LAP the spectral features remained unchanged, but for a decrease in its fluorescence yield. Conversely, *O*-LAP displayed negligible fluorescence inside the cells, pointing to a low intracellular photoactivity.

Cellular phototoxicity

Phototoxicity assay

The phototoxic potential of LAP, *N*-LAP and *O*-LAP was determined using the *in vitro* 3T3 NRU phototoxicity test. To this purpose, cell viability of BALB/c 3T3 fibroblasts treated with increasing concentrations of LAP or its metabolites in dark conditions or in combination with UVA light was measured by neutral red as a vital dye. Half maximal inhibitory concentrations (IC50) under both conditions were estimated from dose-response curves (Fig. S1). The ultimate goal of the NRU assay is to calculate the photoirritation factor (PIF) of a compound, defined as the ratio between its IC50 under dark or light conditions. Chlorpromazine, an anti-psychotic drug with well-known phototoxic properties, was used as a positive control of the assay(Palumbo et al. 2016). The obtained values are collected in Table 1. Parent drug LAP was clearly phototoxic with a PIF value of 21, while *O*-LAP metabolite did not exhibit any phototoxic potential (PIF 1). The lack of phototoxicity *O*-LAP would be related to its lower photoactivity inside the cells, as inferred from its weak fluorescence emission. It is noteworthy that *N*-LAP metabolite retained the phototoxicity of the parent drug with a PIF value of 8. The decrease in the PIF of *N*-LAP could be attributed to an enhanced cytotoxicity of the

metabolite under dark conditions with a 5-fold reduction of the IC_{50} in comparison with LAP.

Protein Photooxidation

As stated above, LAP exerts its pharmacological activity in cancer cells through specific binding to the plasmatic membrane receptors EGFR and HER2, and its transport through the blood system is facilitated by interactions with serum proteins. Indeed, in previous work regarding photophysical studies of LAP, a high binding affinity to human serum albumin (HSA) was reported (Kabir et al. 2016). Hence, the photosensitizing properties of LAP and *N*-LAP towards proteins were investigated using HSA as model. Aqueous mixtures containing HSA and LAP, *N*-LAP, or *O*-LAP were UVA irradiated and the carbonyl moiety, as an early biomarker of oxidative damage, was quantified by 2,4-dinitropheynlhydrazine derivatization method. As shown in Fig.3, irradiated HSA alone contained similar levels of carbonyl moiety as non-irradiated HSA, indicating the suitability of the UVA dose selected. As expected, *O*-LAP did not display any oxidative damage towards HSA. By contrast, both LAP and *N*-LAP significantly increased the carbonyl concentration in HSA after UVA irradiation, clearly suggesting the capability of these compounds to mediate photooxidation in cellular membranes. Noteworthy, this effect was higher for LAP than for *N*-LAP in agreement with the results obtained in the phototoxicity test.

Assessment of photogenotoxicity

Photosensitized Damage to DNA

To investigate whether the phototoxicity displayed by LAP and its *N*-LAP metabolite can also involve damage to DNA bases, photocleavage experiments were performed with supercoiled plasmid pBR322 alone or in combination with DNA-repair enzymes. This assay is based on the conversion of native supercoiled form I into open circular form II upon UVA irradiation in the presence of a photosensitizing drug or metabolite taking advantage of the different electrophoretic mobility of both forms in an agarose gel. To reveal the nature of the base damage, the use of DNA-repair enzymes can be used. Thus, mixtures containing LAP or its metabolites and DNA plasmid pBR322 were irradiated to detect direct single strand brakes (ssb). Remarkably, agarose gel electrophoresis (Fig. S2a) revealed a higher photogenotoxicity for the *N*-LAP metabolite than for the parent drug LAP through formation of the open circular form II quantified by densitometry (Fig. S2b). As anticipated, *O*-LAP metabolite did not display any photogenotoxic effect

towards plasmid pBR322. This result indicates again that LAP metabolism can modulate the potential to photosensitize DNA damage.

In another set of experiments, several DNA-repair enzymes T4 endonuclease V (Endo V), endonuclease III (Endo III) and formamidopyrimidine DNA glycosylase (FPG) were used to reveal cyclobutane thymine dimers, degradation products of pyrimidine bases and oxidized purines, respectively. As shown in Fig.4, quantification by densitometry of form II plasmid showed that ssb formation was not significantly influenced by the Endo V (Fig.4a) and Endo III (Fig. 4b) enzymes. Interestingly, ssb formation in the presence of FPG repair-enzyme was clearly enhanced only for the *N*-LAP metabolite (Fig.4c), thus pointing to the selective generation of oxidatively damaged of purine bases in DNA by this metabolite upon UVA irradiation.

Evaluation of Cellular DNA Damage

In a cellular milieu, there are a large number of biomolecules and metabolites that could have a strong influence on the effect displayed by an added compound. Thus, photogenotoxicity was investigated in a cellular environment using single-cell gel electrophoresis or comet assay under alkaline conditions. This technique allows detecting strand breaks (single or double) as well as alkali-labile sites on chromosomic DNA of an individual cell. Thus, human dermal fibroblasts (FSK) were incubated for 1 h with LAP or its metabolites. After UVA exposure, cells were embedded in agarose on a slide, subjected to lysis, and then, electrophoresis was performed so that the damaged DNA could migrate away from the nucleus. Upon staining with SYBR Gold, the fluorescence patterns of the comet nucleoids and tails were analyzed, and the percentage of DNA damage calculated according to the classification of the images in six different categories. Comet assay evidenced that LAP in combination with UVA light promoted mild damage (around 30%) to cellular DNA (Fig.5) as fragmented DNA moved faster through agarose gel towards the anode, forming a tail (Inset Fig.5 and Fig. S3)

This result could be explained by the higher sensitivity of the comet assay to detect DNA damage. By contrast, *O*-LAP metabolite did not show any photogenotoxicity as the nucleoids remained intact and resembled those from control cells, in agreement with the negative results obtained in previous assays. Once more, *N*-LAP metabolite displayed again higher photogenotoxicity than the parent drug LAP, with comets containing an enhanced DNA fluorescence in the tail (*ca*. 65% of DNA damage).

Oxidative DNA damage comprises a multitude of lesions, many of which are mutagenic and ultimately may lead to the development of photocarcinogenesis (Cadet and Davies

2017). One of the most widely studied lesions is the formation of 8-Oxo-dG (8-Oxo-7,8-dihydro-2'-deoxyguanosine) as a consequence of guanine base oxidation. To confirm the higher oxidative potential towards DNA promoted by *N*-LAP, 8-Oxo-dG production was measured in FSK cells using a competitive enzyme-linked immunosorbent assay (ELISA assay). Accordingly, after UVA irradiation, DNA from samples was isolated, and its quality and concentration were determined by UV spectroscopy in order to rule out extensive unspecific DNA degradation during the irradiation step. The 8-Oxo-dG concentration was calculated by interpolation from the calibration curve using a commercial standard. The results are shown in Fig. 6 and they revealed that after irradiation, the levels of 8-Oxo-dG in DNA of FSK cells significantly increased about 2-fold for the *N*-LAP metabolite, whereas for the parent drug and *O*-LAP metabolite they remained constant, in line with the enzyme-repair plasmid experiments. Thus, the obtained data confirmed again that oxidative DNA damage towards purine bases plays a significant role in the photogenotoxicity exhibited by *N*-LAP metabolite.

Conclusion

In conclusion, the present work has proven that not only LAP but also its metabolite *N*-LAP have the capability to induce photosensitivity disorders. They are both phototoxic and photogenotoxic to cells, as revealed by the 3T3 NRU assay and the comet assay, respectively. By contrast, the O-dealkylated metabolite *O*-LAP does not display relevant photobiological properties. Interestingly, the parent drug LAP shows the highest activity in membrane phototoxicity and protein oxidation, whereas *N*-LAP is associated with the highest photogenotoxicity, through oxidation of purine bases, as revealed by detection of 8-Oxo-dG. Overall, these results are relevant in connection with photosafety issues and highlight the role of drug metabolism in photobiological risk assessment.

Conflict of interest

The authors declare that they have no conflict of interest.

References

Abo-Zeid MAM, Abo-Elfadl MT, Gamal-Eldeen AM (2019) Evaluation of lapatinib cytotoxicity and genotoxicity on MDA-MB-231 breast cancer cell line. Environ Toxicol Pharmacol 71:103207 doi:10.1016/j.etap.2019.103207

Agundez JAG, Garcia-Martin E, Garcia-Lainez G, Miranda MA, Andreu I (2020) Photomutagenicity of chlorpromazine and its N-demethylated metabolites assessed by NGS. Sci Rep 10(1):6879 doi:10.1038/s41598-020-63651-y

Cadet J, Davies KJA (2017) Oxidative DNA damage & repair: An introduction. Free Radic Biol Med 107:2-12 doi:10.1016/j.freeradbiomed.2017.03.030

Castellino S, O'Mara M, Koch K, Borts DJ, Bowers GD, MacLauchlin C (2012) Human metabolism of lapatinib, a dual kinase inhibitor: implications for hepatotoxicity. Drug Metab Dispos 40(1):139-50 doi:10.1124/dmd.111.040949

Ding J, Yao Y, Huang G, et al. (2020) Targeting the EphB4 receptor tyrosine kinase sensitizes HER2-positive breast cancer cells to Lapatinib. Cancer Lett 475:53-64 doi:10.1016/j.canlet.2020.01.032

Ferlay J, Soerjomataram I, Dikshit R, et al. (2015) Cancer incidence and mortality worldwide: sources, methods and major patterns in GLOBOCAN 2012. Int J Cancer 136(5):E359-86 doi:10.1002/ijc.29210

Frenel J-S, Bourbouloux E, Berton-Rigaud D, Sadot-Lebouvier S, Zanetti A, Campone M (2009) Lapatinib in Metastatic Breast Cancer. Women's Health 5(6):603-612 doi:10.2217/whe.09.54

Garcia-Lainez G, Martinez-Reig AM, Limones-Herrero D, Consuelo Jimenez M, Miranda MA, Andreu I (2018) Photo(geno)toxicity changes associated with hydroxylation of the aromatic chromophores during diclofenac metabolism. Toxicol Appl Pharmacol 341:51-55 doi:10.1016/j.taap.2018.01.005

Gavilá J, De La Haba J, Bermejo B, et al. (2020) A retrospective, multicenter study of the efficacy of lapatinib plus trastuzumab in HER2-positive metastatic breast cancer patients previously treated with trastuzumab, lapatinib, or both: the Trastyvere study. Clinical and Translational Oncology 22(3):420-428 doi:10.1007/s12094-019-02145-4

Geyer CE, Forster J, Lindquist D, et al. (2006) Lapatinib plus Capecitabine for HER2-Positive Advanced Breast Cancer. New England Journal of Medicine 355(26):2733-2743 doi:10.1056/NEJMoa064320

Gomez HL, Doval DC, Chavez MA, et al. (2008) Efficacy and safety of lapatinib as first-line therapy for ErbB2-amplified locally advanced or metastatic breast cancer. J Clin Oncol 26(18):2999-3005 doi:10.1200/JCO.2007.14.0590

Heppt MV, Clanner-Engelshofen BM, Marsela E, et al. (2020) Comparative analysis of the phototoxicity induced by BRAF inhibitors and alleviation through antioxidants. Photodermatol Photoimmunol Photomed 36(2):126-134 doi:10.1111/phpp.12520

Higa GM, Abraham J (2007) Lapatinib in the treatment of breast cancer. Expert review of anticancer therapy 7(9):1183-92 doi:10.1586/14737140.7.9.1183

Huijberts SCFA, van Geel RMJM, van Brummelen EMJ, et al. (2020) Phase I study of lapatinib plus trametinib in patients with KRAS-mutant colorectal, non-small cell lung, and pancreatic cancer. Cancer Chemotherapy and Pharmacology 85(5):917-930 doi:10.1007/s00280-020-04066-4

Kabir MZ, Mukarram AK, Mohamad SB, Alias Z, Tayyab S (2016) Characterization of the binding of an anticancer drug, lapatinib to human serum albumin. J Photochem Photobiol B 160:229-39 doi:10.1016/j.jphotobiol.2016.04.005

Kopper L (2008) Lapatinib: A Sword With Two Edges. Pathology & Oncology Research 14(1):1-8 doi:10.1007/s12253-008-9018-z

Medina PJ, Goodin S (2008) Lapatinib: a dual inhibitor of human epidermal growth factor receptor tyrosine kinases. Clin Ther 30(8):1426-47 doi:10.1016/j.clinthera.2008.08.008

Mendelsohn J, Baselga J (2000) The EGF receptor family as targets for cancer therapy. Oncogene 19(56):6550-65 doi:10.1038/sj.onc.1204082

Moon JY, Han JM, Seo I, Gwak HS (2019) Risk factors associated with the incidence and time to onset of lapatinib-induced hepatotoxicity. Breast Cancer Research and Treatment 178(1):239-244 doi:10.1007/s10549-019-05382-x

Nolting M, Schneider-Merck T, Trepel M (2014) Lapatinib. Recent results in cancer research Fortschritte der Krebsforschung Progres dans les recherches sur le cancer 201:125-43 doi:10.1007/978-3-642-54490-3_7

OECD (2004) Guidelines for the Testing of Chemicals Test No. 432: In Vitro 3T3 NRU Phototoxicity Test. In: Development OfECa (ed).

Palumbo F, Garcia-Lainez G, Limones-Herrero D, et al. (2016) Enhanced photo(geno)toxicity of demethylated chlorpromazine metabolites. Toxicol Appl Pharmacol 313:131-137 doi:10.1016/j.taap.2016.10.024

Parham LR, Briley LP, Li L, et al. (2016) Comprehensive genome-wide evaluation of lapatinib-induced liver injury yields a single genetic signal centered on known risk allele HLA-DRB1*07:01. The Pharmacogenomics Journal 16(2):180-185 doi:10.1038/tpj.2015.40

Rayane Mohamed FS, Jonathan Sidibe, Nasim Bararpour, Jules Desmeules, Marc Ausburger, Youssef Daali and A Thomas (2018) Detection and Identification of Reactive Drug Metabolites Leading to Idiosyncratic Toxicity: Lapatinib as a Case Example. Journal of Drug Metabolism & Toxicology 9(3):1-6 doi:10.4172/2157-7609.1000242Schroeder RL, Stevens CL, Sridhar J (2014) Small molecule tyrosine kinase inhibitors of ErbB2/HER2/Neu in the treatment of aggressive breast cancer. Molecules 19(9):15196-212 doi:10.3390/molecules190915196

Spector N, Xia W, El-Hariry I, Yarden Y, Bacus S (2007) HER2 therapy. Small molecule HER-2 tyrosine kinase inhibitors. Breast Cancer Research 9(2):205 doi:10.1186/bcr1652

Spraggs CF, Budde LR, Briley LP, et al. (2011) HLA-DQA1*02:01 Is a Major Risk Factor for Lapatinib-Induced Hepatotoxicity in Women With Advanced Breast Cancer. Journal of Clinical Oncology 29(6):667-673 doi:10.1200/jco.2010.31.3197

Tokura Y, Ogai M, Yagi H, Takigawa M (1994) Afloqualone photosensitivity: immunogenicity of afloqualone-photomodified epidermal cells. Photochem Photobiol 60(3):262-7 doi:10.1111/j.1751-1097.1994.tb05102.x

Towles JK, Clark RN, Wahlin MD, Uttamsingh V, Rettie AE, Jackson KD (2016) Cytochrome P450 3A4 and CYP3A5-Catalyzed Bioactivation of Lapatinib. Drug Metab Dispos 44(10):1584-97 doi:10.1124/dmd.116.070839

Wang H (2014) Lapatinib for the treatment of breast cancer in the People's Republic of China. Onco Targets Ther 7:1367-73 doi:10.2147/OTT.S60586

Table 1. *In vitro* 3T3 NRU Phototoxicity Assay of LAP and its metabolites

Compound	**IC_{50} Dark (µM)**	**IC_{50} UVA Light (µM)**	**Photoirritant Factor (PIF)[1]**
CPZ	67 ± 9	3.7 ± 0.4	18
LAP	21 ± 4	1.0 ± 0.3	21
O-LAP	189 ± 42	231 ± 39	1
N-LAP	4.0 ± 0.7	0.5 ± 0.1	8
SDS	202 ± 25	244 ± 48	1

Data represent the mean ± SD from five independent dose-responses curves. CPZ and SDS were selected as positive and negative controls of phototoxicity, respectively. [1]According to the OECD 432 Guide (2004), PIF<2 means "no phototoxicity", 2<PIF<5 means "probable phototoxicity" and PIF>5 means "phototoxicity".

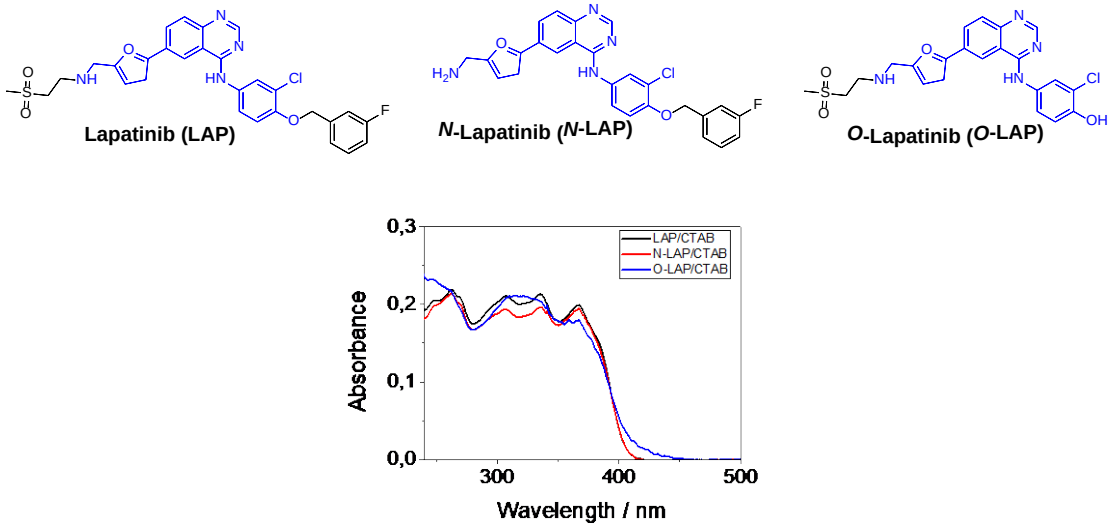

Fig. 1 a) Chemical structure of Lapatinib (LAP), *N*-Lapatinib (*N*-LAP) and *O*-Lapatinib (*O*-LAP). b) Absorption spectra of LAP and its metabolites in CTAB micelles in aqueous solutions at 5 µM.

a)

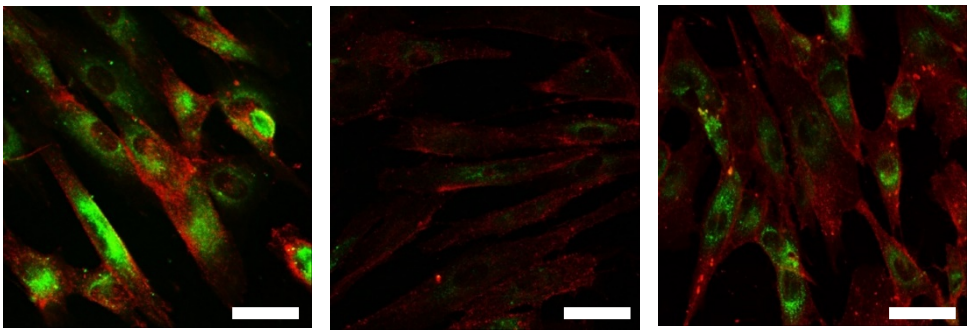

b)

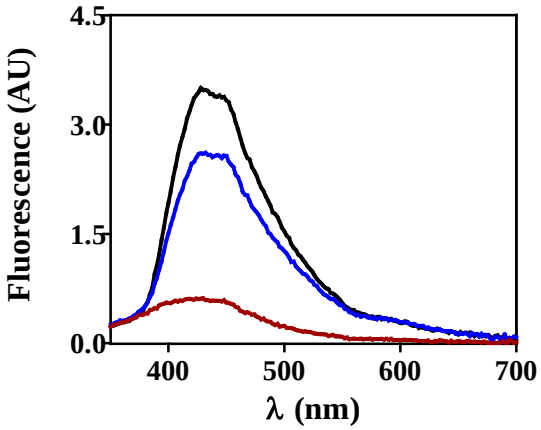

Fig. 2 a) Intracellular localization of LAP (left), *O*-LAP (middle) and *N*-LAP (right) in FSK by confocal microscopy. Fibroblasts seeded on glass coverslips were incubated with 5 µM solutions of LAP, *O*-LAP or *N*-LAP (green fluorescence) and further labeled with CellMaskTM Orange Plasma membrane (red fluorescence). A cytoplasmic distribution is observed for all compounds. White bars represent 50 µm. b) Fluorescence emission spectra (λ_{exc}= 320 nm) of LAP (**black**), *N*-LAP (**blue**) and *O*-LAP (**red**) after internalization on FSK cells.

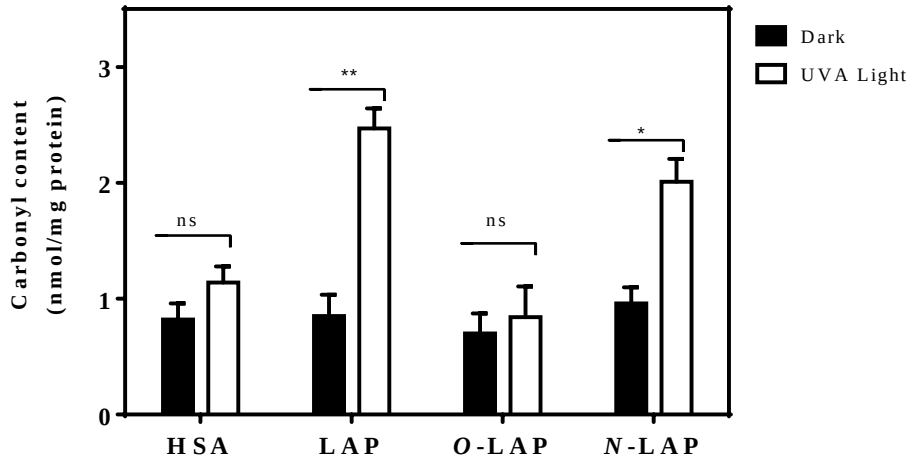

Fig. 3 Protein photooxidation by LAP and its metabolites. HSA solutions in PBS (5mg/mL), alone (HSA) or in the presence of 30 µM of LAP, *O*-LAP or *N*-LAP were irradiated with an UVA dose of 15 J/cm^2 (□, UVA Light) or kept in the dark conditions (■). Protein oxidation was spectrophotometrically evaluated by monitoring its carbonyl moiety after derivatization with 2,4-dinitrophenylhydrazine (DNPH). Data are the mean ± SD of three independent experiments. Asterisks indicate significant differences relative to the carbonyl content in HSA in darkness by the t-Student test (*p<0.05, *p<0.01, ns: non-significant).

a)

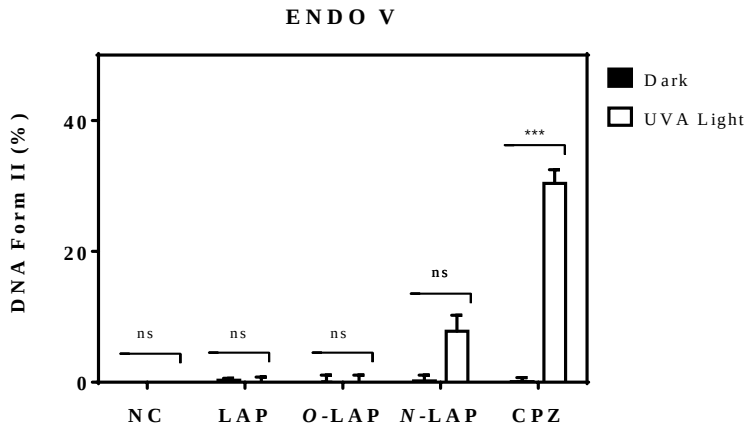

b)

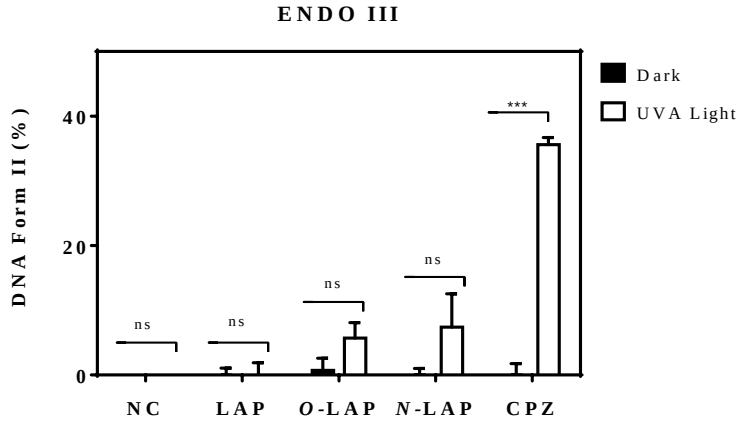

c)

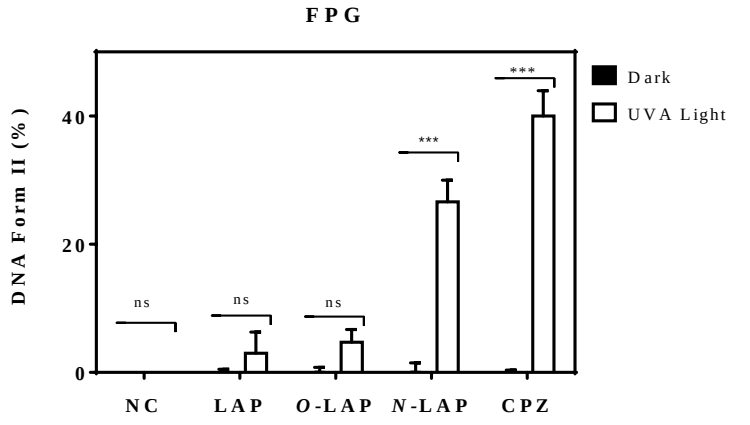

Fig. 4 Percentage of DNA Form II formation by means of restriction enzyme digestion (Endo V (a), Endo III (b) or FPG (c)) of pBR322 (250 ng) incubated with LAP or its metabolites (30 µM) in the presence (□) or absence (■) of UVA Light (15 J/cm^2). Data are the mean ± SD of four independent experiments. The initial value of Form II was subtracted from all samples. Asterisks indicate significant differences relative to the formation of DNA Form II in darkness by the t-Student test (ns: non-significant, ***$p<0.001$). CPZ was used as positive control of photogenotoxicity.

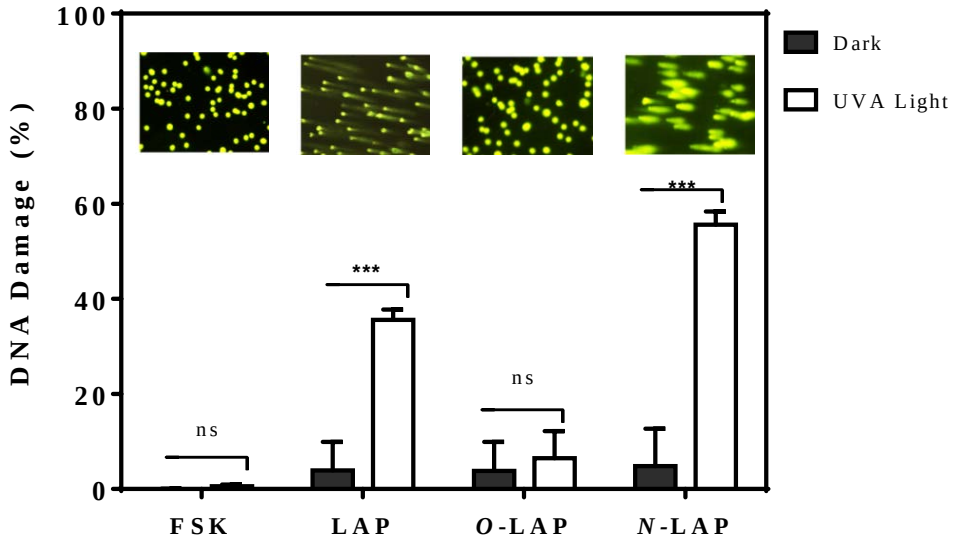

Fig. 5 Nuclear DNA photodamage promoted by LAP, *N*-LAP and *O*-LAP assessed by alkaline comet assay**.** Data are reported as the percentage of DNA damage calculated by visual scoring of untreated cells (FSK) or treated with LAP or its metabolites *O*-LAP and *N*-LAP (30 μM). Cells were kept on dark conditions (Dark, ■) or irradiated with a 2.5 J/cm^2 UVA dose (UVA Light, □). Data represent the mean±SD of three independent experiments. Asterisks indicate significant differences by the t-Student test (***$p<0.001$, ns: non-significant). Inset: Representative microscopy images of irradiated non-treated cells or treated with LAP, *O*-LAP and *N*-LAP.

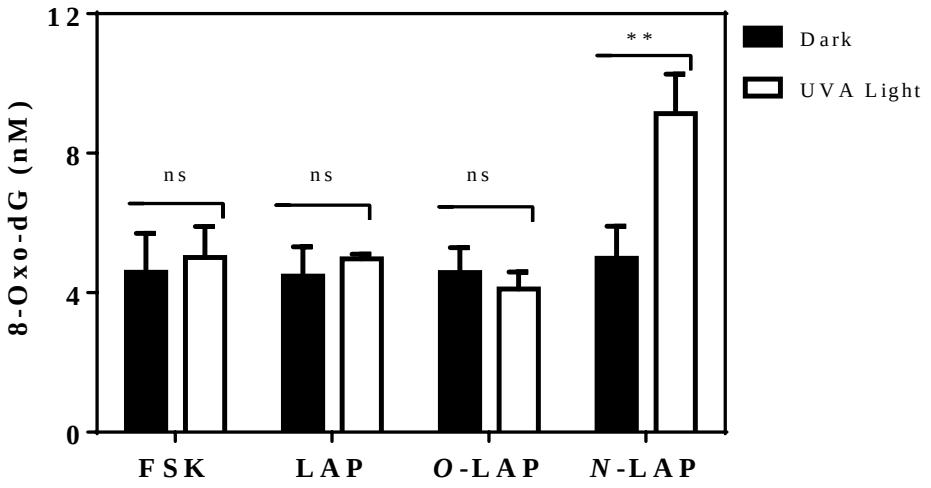

Fig. 6 Oxidation photodamage at purine base upon LAP and its metabolites treatment. 8-Oxo-dG formation in genomic DNA upon treatment with LAP or its metabolites (*O*-LAP and *N*-LAP) in FSK cells. Cells were incubated with LAP, *O*-LAP or *N*-LAP (30 μM) and left unexposed (Dark, ■), or irradiated with a 2.5 J/cm^2 UVA dose (UVA Light, □). Then, DNA was isolated and the concentration of 8-Oxo-dG was quantified in all samples by means of a colorimetric ELISA assay. Data are the mean ± SD of three independent experiments. Asterisks denote significant differences by the t-Student test (**$p < 0.01$; ns: non-significant).